#3

NAVY DEPARTMENT

THE DAVID W. TAYLOR MODEL BASIN

WASHINGTON 7, D.C.

[redacted]

THE USE OF DOUBLY REFRACTING SOLUTIONS IN THE INVESTIGATION OF FLUID FLOW PHENOMENA

by

Benjamin Rosenberg

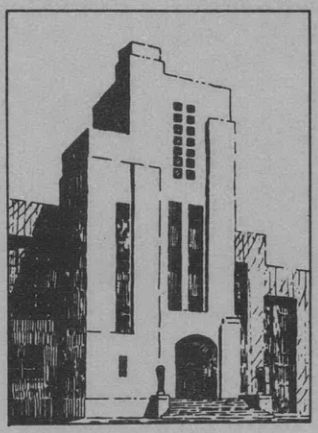

March 1952

Report 617

INITIAL DISTRIBUTION

Copies

17 Chief, BuShips, Project Records (Code 324), for distribution:
- 5 Project Records
- 3 Research (Code 300)
- 2 Applied Science (Code 370)
- 2 Design (Code 410)
- 2 Preliminary Design (Code 420)
- 1 Propellers and Shafting (Code 554)
- 1 Technical Assistant to Chief of the Bureau (Code 106)
- 1 Submarines (Code 515)

4 Chief of Naval Research, for distribution:
- 3 Fluid Mechanics (N426)
- 1 Undersea Warfare (466)

4 Commander, U.S. Naval Ordnance Laboratory, Mechanics Division, White Oak, Silver Spring 19, Md.

4 Commander, Naval Ordnance Test Station, Inyokern, China Lake, Calif.

1 Commander, Portsmouth Naval Shipyard, Portsmouth, N.H.

1 Commanding Officer, Navy Underwater Sound Laboratory, Fort Trumbull, New London, Conn.

5 Chief, BuOrd, Underwater Ordnance (Re6a)

3 Chief, BuAer, Aerodynamics and Hydrodynamics Branch (DE-3)

1 Director, Technical Information Branch, Aberdeen Proving Grounds, Aberdeen, Md.

6 Director, National Advisory Committee for Aeronautics, 1724 F St., N.W., Washington, D.C.

2 Newport News Shipbuilding and Dry Dock Co., Newport News, Va., for distribution:
- 1 Senior Naval Architect
- 1 Supervisor, Hydraulics Laboratory

1 Director, Institute of Aeronautical Sciences, 2 East 64th St., New York 21, N.Y.

1 Director, Institute for Mathematics and Mechanics, New York University, 45 Fourth Ave., New York 3, N.Y.

2 Director, Experimental Naval Tank, Department of Naval Architecture and Marine Engineering, University of Michigan, Ann Arbor, Mich.

1 Chairman, Department of Aeronautical Engineering, New York University, University Heights, New York 53, N.Y.

1 Head, Technical Reference Section, U.S. Department of Interior, Bureau of Reclamation, Denver Federal Center, Denver, Colo.

1 Administrator, Webb Institute of Naval Architecture, Crescent Beach Road, Glen Cove, Long Island, N.Y.

1 Director, U.S. Waterways Experiment Station, Vicksburg, Miss.

1 Director, Applied Physics Laboratory, Johns Hopkins University, 8621 Georgia Avenue, Silver Spring, Md.

2 Director, Ordnance Research Laboratory, Pennsylvania State College, State College, Pa.

Copies	
1	Superintendent, U.S. Naval Postgraduate School, Monteray, Calif.
1	Department of Civil Engineering, Colorado A and M College, Fort Collins, Colo.
2	Director, Hydrodynamic Laboratory, California Institute of Technology, Pasadena 4, Calif.
1	Director, Woods Hole Oceanographic Institution, Woods Hole, Mass.
2	Director, Experimental Towing Tank, Stevens Institute of Technology, 711 Hudson Street, Hoboken, N.J.
2	Head, Department of Naval Architecture and Marine Engineering, Massachusetts Institute of Technology, Cambridge 39, Mass.
2	Director, Institute for Fluid Dynamics and Applied Mathematics, University of Maryland, College Park, Md., 1 for Dr. Weinstein
1	Librarian, American Society of Mechanical Engineers, 29 West 39th St., New York 18, N.Y.
1	Librarian, American Society of Civil Engineers, 33 West 39th Street, New York 18, N.Y.
1	Librarian, Daniel Guggenheim Aeronautical Laboratory, California Institute of Technology, Pasadena 4, Calif.
1	Editor, Aeronautical Engineering Review, 2 East 64th St., New York 21, N.Y.
2	Editor, Applied Mechanics Reviews, Midwest Research Institute, 4049 Pennsylvania, Kansas City 2, Mo.
1	Editor, Bibliography of Technical Reports, Office of Technical Services, U.S. Department of Commerce, Washington 25, D.C.
1	Editor, Technical Data Digest, Central Air Documents Office, Wright-Patterson Air Force Base, Dayton, Ohio
1	Division of Applied Mathematics, Brown University, Providence, R.I.
1	Department of Civil Engineering, Columbia University, New York 27, N.Y.
2	Dr. Hunter Rouse, Director, Iowa Institute of Hydraulic Research, State University of Iowa, Iowa City, Iowa
1	Dr. R.T. Knapp, Hydrodynamic Laboratory, California Institute of Technology, Pasadena 4, Calif.
2	Dr. L.G. Straub, Director, St. Anthony Falls Hydraulic Laboratory, University of Minnesota, Minneapolis 14, Minn.
2	Dr. V.L. Streeter, Illinois Institute of Technology, 3300 Federal Street, Chicago 16, Ill.
1	Dr. C.C. Lin, Department of Mathematics, Massachusetts Institute of Technology, Cambridge 39, Mass.
1	Prof. W.S. Hamilton, Technical Institute, Northwestern University, Evanston, Ill.
1	Prof. G. Birkhoff, Harvard University, Cambridge, Mass.
1	Prof. K.E. Schoenherr, School of Engineering, Notre Dame University, Notre Dame, Ind.
1	Prof. W. Spannhake, Armour Research Foundation, 35 West 33rd Street, Chicago 16, Ill.

Copies

1 Dr. J.V. Wehausen, Editor, Mathematical Reviews, 80 Waterman St., Providence, R.I.

1 Dr. D. Gilbarg, Department of Mathematics, Indiana University, Bloomington, Ind.

2 Prof. J. Vennard, Department of Civil Engineering, Stanford University, Palo Alto, Calif.

1 Dr. G.F. Wislicenus, Mechanical Engineering Department, Johns Hopkins University, Baltimore 18, Md.

1 Dr. G.B. Schubauer, National Bureau of Standards, Washington, D.C.

1 Prof. R.A. Dodge, Engineering Mechanics Department, University of Michigan, Ann Arbor, Mich.

2 Dr. A.T. Ippen, Director, Hydrodynamics Laboratory, Department of Civil and Sanitary Engineering, Massachusetts Institute of Technology, Cambridge 39, Mass.

1 Dr. C.A. Wright, Department of Hydraulic and Sanitary Engineering, Polytechnic Institute of Brooklyn, 99 Livingston St., Brooklyn 2, N.Y.

1 Prof. R.G. Folsom, Department of Engineering, University of California, Berkeley 4, Calif.

1 Prof. C.W. Harris, Department of Civil Engineering, University of Washington, Seattle 5, Wash.

1 Prof. S.A. Guerrieri, Division of Chemical Engineering, University of Delaware, Newark, Del.

1 Prof. J.L. Hooper, Alden Hydraulic Laboratory, Worcester Polytechnic Institute, Worcester, Mass.

1 Prof. R.C. Binder, Department of Mechanical Engineering, Purdue University, Lafayette, Ind.

1 Dr. M.S. Plesset, California Institute of Technology, Pasadena 4, Calif.

1 Dr. A.G. Strandhagen, School of Engineering, Notre Dame University, Notre Dame, Ind.

1 Dr. V.L. Schiff, Stanford University, Palo Alto, Calif.

1 Mr. C.A. Lee, Hydraulic Engineer, Research and Development Laboratories, Kimberly-Clark Corp., Neenah, Wis.

1 Mr. Paul F. Ruff, 13216 Thornhurst Ave., Cleveland 5, Ohio

1 Mr. J.P. Breslin, Gibbs and Cox, Inc., 21 West Street, New York 6, N.Y.

1 Mr. Floyd Hasselris, Department of Mechanical Engineering, The Cooper Union, Cooper Square, New York 3, N.Y.

1 Dr. Th. von Kármán, 1051 South Marengo St., Pasadena, Calif.

9 British Joint Services Mission, Navy Staff, P.O. Box 165, Benjamin Franklin Station, Washington, D.C.

2 Director, Hydrodynamics Laboratory, National Research Council, Ottawa, Canada

1 Prof. J.K. Lunde, Skipsmodelltanken, Tyholt Trondheim, Norway

Copies

1 Prof. L. Troost, Superintendent, Netherlands Ship Model Basin, Haagsteeg 2, Wageningen, The Netherlands

1 Directeur du Bassin d'Essais Des Carènes, 6, Boulevard Victor, Paris XV, France

1 Director, Swedish State Shipbuilding Experimental Tank, Göteborg 24, Sweden

1 Dr. G. Hughes, National Physical Laboratory, Teddington, Middlesex, England

1 Editor, Journal of the British Shipbuilding Research Association, 5 Chesterfield Gardens, Curzon St., London W. 1, England

1 Editor, Physics Abstracts, Institution of Electrical Engineers, Savoy Place, London W.C. 2, England

1 Editor, Index Aeronauticus, Ministry of Supply, Millbank, London S.W. 1, England

1 Head, Aerodynamics Division, National Physical Laboratory, Teddington, Middlesex, England

1 Head, Aerodynamics Department, Royal Aircraft Establishment, Farnborough, Hants, England

1 Head, Aeronautics Department, Imperial College, London, S.W. 7, England

1 Head, College of Aeronautics, Cranfield, Bletchley, Bucks, England

1 Prof. J. Kampé de Fériet, Faculté des Sciences, Université de Lille, Lille (Nord), France

1 Directeur, Laboratoire Dauphinois d'Hydraulique des Ateliers Neyrpic, Avenue de Beauvert, Grenoble (Isère), France

1 Office National d'Études et de Recherches Aéronautiques 3, rue Léon Bonnat, Paris XVI, France

1 Prof. D.P. Riabouchinsky, Centre National de la Recherche Scientifique, 13 Quai d'Orsay, Paris VII, France

1 Prof. J.M. Burgers, Laboratorium Voor Aero-En Hydrodynamica, Nieuwe Laan 76, Delft, The Netherlands

1 Dr. R. Timman, National Luchtvaartlaboratorium, Sloterwag 145, Amsterdam, The Netherlands

1 Director, Aeronautical Research Institute of Sweden, Ranhammarsvagen 12, Ulsvunda, Sweden

1 Prof. J. Ackeret, Institut für Aerodynamik Der Eidgenössiche Technische Hochschule, Zürich, Switzerland

1 Dr. L. Malavard, Office National d'Études et de Recherches Aéronautiques, Chatillon, Paris, France

TABLE OF CONTENTS

NOTATION

a,b	Horizontal and vertical components of amplitude of vibration
D_v	Viscous drag
F	Photoelastic optical constant
g	Acceleration due to gravity
h	Channel depth
l	Thickness of specimen or test section
M	Maxwell constant
N	Fringe order
n	Distance measured along normal to streamline
p	Pressure
Q	Rate of discharge
r	Radius at any point between cylinders ($r_i \leq r \leq r_o$)
r_i	Outer radius of inner cylinder
r_o	Inner radius of outer cylinder
S	Sensitivity of solution
s	Distance measured along streamline
T	Period
t	Time
u,v,w	Velocity components in x,y and z directions respectively
V	Velocity of fluid
α	Acute angle measured from a plane of maximum shear to the tangent to the streamline
β	Angle measured from the reference plane to the streamline
γ	Specific weight, force per unit volume
δ	Light path difference in wave lengths
ϵ	Angle from the optic axis to the plane of polarization
ζ	Isoclinic angle; angle from the reference plane to the optic axis of the particle
η	Angle from the horizontal to the plane of maximum shear
θ	Polar angle; angle from positive z-axis to long axis of particle
λ	Wavelength
μ	Coefficient of viscosity
ν	Kinematic viscosity
ξ	Angle from the direction of undisturbed motion to the plane tangent to the surface of the model at any point
ρ	Radius of curvature of streamline
τ_{max}	Maximum shear stress
τ_{xy}	Shear stress in horizontal plane

ϕ	Azimuthal angle; acute angle measured from XZ-plane to meridian plane, ZOP, of particle
χ	Extinction angle; acute angle between optic axis and streamline
ψ	Stream function (subscripts indicate coordinates where ψ is evaluated)
ω	Angular velocity

THE USE OF DOUBLY REFRACTING SOLUTIONS IN THE INVESTIGATION OF FLUID FLOW PHENOMENA

by

Benjamin Rosenberg

ABSTRACT

The feasibility of using doubly refracting liquids for qualitative and quantitative flow studies is discussed. Of the many liquids which have the property of streaming double refraction, colloidal solutions of bentonite are most suitable because of their high sensitivity, low viscosity, cheapness, and comparative ease of preparation. The problems involved in the preparation and handling of bentonite solutions and the physical factors affecting the double refracting properties of bentonite, such as concentration, particle size, and temperature are investigated.

An outline of the essential optical theory and of the application of double refraction methods in photoelasticity is presented. The methods of generating and measuring double refraction are described and an optical setup suitable for hydrodynamic studies is recommended.

A thorough survey of existing literature concerning streaming double refraction for colloidal solutions and pure liquids is made. This includes the hydrodynamic theories developed. A method of determining the velocity distribution and streamlines for two-dimensional laminar flow utilizing ideas obtained from the literature is suggested. However, the adequacy of the hydrodynamic theory as applied to colloidal particles in two-dimensional flow is open to question. Therefore a more complete analysis is attempted. These results indicate the need for special experiments in order to determine the proper relationships between double refraction and velocity gradients. A method for determining the velocity distribution and streamlines using pure liquids possessing birefringent properties is also presented.

Once the velocity distribution and streamlines have been obtained, methods of obtaining the pressure distribution, viscous drag, and viscous lift are suggested.

Finally, the feasibility of utilizing streaming birefringence for studying three-dimensional and turbulent flow is discussed briefly.

INTRODUCTION

The development of qualitative and quantitative methods for study of the flow around underwater bodies has been a subject of intensive investigation. Visual methods such as dye streaks, aluminum particles and smoke are useful but give few quantitative results. Pressure and velocity measurements by means of pitot probes are very laborious and require the use of instruments which, although small, do affect the flow. Therefore, a visual method which can be used quantitatively would be very advantageous.

In common with other colloids, bentonite ($Al_2O_3 \cdot 4SiO_2 xH_2O$) exhibits the property of streaming double refraction. This effect may be due to two causes: (a) orientation of the particles by viscous shear forces and (b) deformation of the particles.[1,2] The amount of double refraction (birefringence) is dependent directly upon the shear rate (velocity gradient).[3,4,5] For present purposes bentonite is superior to many other colloids such as ferric oxide, vanadium pentoxide, ethyl cellulose, etc. This is due in the main to the fact that the viscosity and surface tension of a dilute bentonite sol are close to that of water, its cost of preparation is not excessive, and it has pronounced optical properties even at elevated temperatures.[6]

For the purpose of studying flow by means of bentonite solutions, a facility is now under construction at the David Taylor Model Basin. This facility will circulate bentonite solutions and is designed to permit a uniform velocity distribution at the entrance to the test section at speeds up to 20 feet per second.

The present paper is limited almost entirely to a discussion of the problems involved in handling and utilizing bentonite solutions, a comprehensive study of the literature pertaining to double refraction of flowing colloidal solutions and pure liquids, and possible methods of utilizing doubly refracting solutions to study the velocity and pressure distribution around underwater bodies moving in a viscous, incompressible liquid in laminar, two-dimensional flow.

BENTONITE SOLUTIONS

The sensitivity S of a doubly refractive solution is defined as the birefringence (double refraction) resulting from a unit shear stress and unit length of light path normal to the flow. The actual measurement of birefringence will be discussed in a later section. Many factors influence the sensitivity of the bentonite sol; these include the type of bentonite used, the

[1]References are listed on page 36.

method of preparation of the sol, and many physical factors such as concentration, temperature, etc.

SUGGESTED METHOD OF PREPARATION

A good grade of Wyoming or California bentonite can be purchased by the pound.[3] After some preliminary pulverizing a suspension of about 4 to 5 percent concentration (by weight) should be prepared by adding the bentonite to distilled water with continuous agitation. Particles greater than colloidal size can be settled out by gravity or by slight centrifuging.[7] A nearly pure sol of uniform particle size can then be prepared.[8,9] The sol should first be diluted to a 2 to 3 percent concentration and then run through a super-centrifuge at a rate of feed of 750 cc per minute and with a centrifuge speed of 22,000 rpm. The clay fraction deposited on the liner is discarded and the overflow is used for the tests.

The initial studies in the TMB Bentonite Channel will be made with a specially prepared solution of California bentonite (Hectorite) provided by the laboratories of the Massachusetts Institute of Technology.

IMPORTANT PHYSICAL FACTORS

There are a number of factors which influence the working characteristics of a bentonite sol. Therefore, knowledge of their effects and methods of control are extremely important.

Particle Size

Bentonite is geometrically anisotropic, the length, width, and height of the crystals being different. The crystals consist of laminated plates, the finest of which are 100 to 300 mμ* long and about 1 mμ thick. Due to the difficulties in obtaining the actual dimensions except by tedious examination under the electron microscope, the size is usually given in terms of apparent or equivalent spherical diameter (e.s.d.). This is the diameter of a spherical particle which would have the same sedimentation velocity as the anisotropic particles being studied. The e.s.d. for bentonite varies from 5 to 200 mμ (Reference 10).

The phenomenon of double refraction in bentonite sols is produced primarily by particles not less than 100 mμ in length or 15 mμ e.s.d.[11] An e.s.d. of about 50 mμ gives the best results. The bentonite can be fractionated to any desired particle size by the centrifuging method described by Hauser and Lynn.[7]

*1 mμ = 1 millimicron = 10^{-7} cm.

Concentration

An increase in the concentration of bentonite sols increases the viscosity, relaxation time, and sensitivity.[12] In order to prevent the possibility of coagulation and yield effects, a maximum concentration of about 0.8 percent by weight is advisable in narrow test sections. In wider test sections, the concentration may have to be further reduced because of the reduction in intensity of the transmitted light due to the longer light path. A concentration of 0.8 percent has a viscosity, surface tension, and density close to that of water, also a high sensitivity and good light transmission qualities. The concentration can be determined by weighing a fixed volume of the solution, then drying to constant weight at 250° F. and weighing the residue. This is the optimum temperature for driving off the water of the solution without dehydrating the bentonite.

Temperature

Changes in temperature affect the viscosity and sensitivity of bentonite sols. Therefore, it is important to keep the temperature constant during the course of the tests. Most dilute colloidal solutions show no unusual viscosity characteristics at temperatures over 100° F.[13] This is probably applicable to bentonite sols, but the reduction in sensitivity at this temperature makes it advisable to maintain a lower temperature. One around 75° F. is a good compromise.

Acidity

The acidity of a solution is evaluated in terms of its pH.* Its effect upon some properties of bentonite is not too clear. It does affect viscosity, which is a minimum at a pH of 11.4. The stability of bentonite sols is a maximum at a pH of 5.8 and again at 11.4 and least stable at pH of 9.4 (Reference 10). However, due to simplicity of preparation and its excellent optical properties, a neutral solution (pH = 7) seems most advisable. In the dilute sols used, there is little danger of coagulation.

Aging and Preliminary Treatment

Bentonite sols are thixotropic, that is, their viscosity and sensitivity are affected by the amount of mechanical work done on them. However, this effect is not indefinite in extent; after a certain amount of mechanical work has been done, the characteristics of the sol remain constant as long as

*pH = $\log_{10}$ 1/concentration of hydrogen ions.

it is agitated. Since the change is reversible, the viscosity will increase on standing.[14,15] Whether thixotropic effects do occur in dilute bentonite sols, and if they do, how long it is necessary to wait before equilibrium is reached can best be determined in a viscometer of the rotating-cylinder type. If this phenomenon does occur, it will be necessary to circulate the sol in the channel for a sufficient time before starting the tests.

The effect of aging upon physical properties is not entirely certain. Some experiments[16] indicate that aging has very little effect.

Foreign Materials

Bentonite sols have a tendency to gel in the presence of electrolytes or on most metal surfaces.[12] This effect limits the materials that may be used. Inert materials include stainless steel, chromium, glass, rubber, silver, and some plastics such as lucite and bakelite.

The addition of an electrolyte causes an increase in the viscosity and settling rate and promotes coagulation. Some electrolyte is necessary for the stability of the bentonite, but enough is usually present from its own ions. The addition of 0.01 percent tetrasodium pyrophosphate[3] helps stability.

Pressure

The effect of pressure upon birefringence is unknown, although it can be checked very readily in a Kundt cell. This cell consists of two concentric cylinders rotating with respect to each other, with transparent ends, so that the cell may be filled with the liquid to be studied and polarized light passed normal to the parallel sides. The viscosity will increase slightly with increasing pressure.

Viscosity

For optimum conditions, it is desirable to have a colloidal sol for which the viscosity is close to that of water and is independent of shear rate. The viscosity of bentonite sols varies somewhat with particle size, but is about 1.80 cp. for a 0.8 percent sol of 50 mμ e.s.d. at 25° C as compared with 0.957 cp. for water at the same temperature.[17] However, even dilute solutions may exhibit non-Newtonian characteristics, the viscosity being affected by shear rate.[10,12] A rotary type viscometer is most suitable for determining the viscosity at various shear rates.

Relaxation Time

After a shearing force has been removed, the time necessary for the action of Brownian movement to destroy the orientation set up by the shearing force is known as the "relaxation time." It is chiefly a function of concentration, temperature, particle shape and size. At normal temperatures and at concentrations below 1 percent, the relaxation time is less than 1/100 of a second, and below 0.5 percent it is practically zero. It can be determined by utilizing the "Kerr effect"[12,19] which is the birefringence occurring due to orientation of the particles when placed in an electric or magnetic field. Therefore, if the bentonite sol is placed in a cell located between crossed polaroids and an alternating current is imposed upon the cell, the intensity of the light passing through the analyzer will vary as long as the frequency of the alternating current is low enough for the particles to follow the current fluctuations faithfully. As soon as the frequency becomes too high for the particles to follow the change in current, the intensity becomes steady. The intensity can be measured by means of a photoelectric cell, the photoelectric current being amplified and recorded on the screen of a cathode ray oscillograph. The reciprocal of the minimum frequency at which the light intensity becomes steady is the relaxation time. It is an indication of the ability of the particular sol to follow rapid changes in shear.

OPTICAL STUDIES

The study of the velocity and pressure distribution around underwater bodies by the use of doubly refracting solutions requires a familiarity with certain optical equipment, phenomena, and terms.

POLARIZATION OF LIGHT

Ordinary light can be considered as vibrations of all ranges of amplitude, wavelength, and orientation. Most birefringence studies utilize polarized light. If the vibrations are in a single plane, the light is said to be plane-polarized. If they consist of two sets of mutually perpendicular vibrations of unequal amplitudes, the light is elliptically polarized, while if the amplitudes are equal and 90° out of phase, the light is circularly polarized. Polarized light is usually obtained by utilizing the doubly refracting properties of certain crystals. A crystal used for such a purpose is called a polarizer. In addition, a similar crystal called an analyzer is used to study the character of the polarized light after its passage through a doubly refracting medium.

DOUBLE REFRACTION

When ordinary light is passed through certain crystals such as calcite, the light will break up and emerge as two separate beams. This phenomenon is known as double refraction. It is found that both beams are plane-polarized and at right angles to one another.

Double Refraction of Plane-Polarized Light

The effect of the passage of plane-polarized light through doubly refracting crystals can be treated analytically. In Figure 1, OP represents the amplitude and plane of vibration of a plane-polarized beam traveling perpendicular to the page. OX is the optic axis of the crystal. In the crystal, the plane-polarized vibration will be divided into two components, one parallel to the optic axis of amplitude $a = OP \cos \epsilon$ and the other perpendicular to the optic axis of amplitude $b = OP \sin \epsilon$. Since the rays travel at different velocities, a path difference δ will result from the passage of the beams through the crystal. At emergence the magnitude of the x- and y-components can be represented by

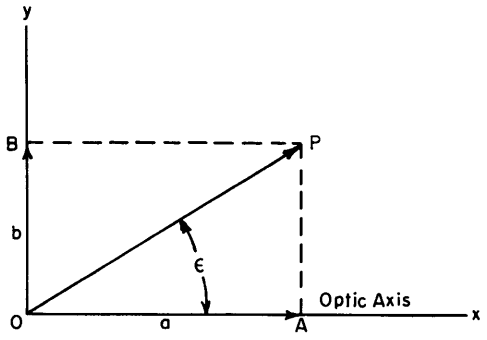

Figure 1 - Sketch Showing Components of Plane-Polarized Beam OP

and

$$x = a \cos 2\pi t/T$$
$$y = b \cos 2\pi \left(t/T + \frac{\delta}{\lambda}\right) \qquad [1]$$

By combining the above equations so as to eliminate t, the resulting equation is

$$\frac{x^2}{a^2} + \frac{y^2}{b^2} - \frac{2xy \cos (2\pi \delta/\lambda)}{ab} = \sin^2 \frac{2\pi\delta}{\lambda} \qquad [2]$$

Since this is the equation for an ellipse, the resultant beam will, in general, be elliptically polarized. In special cases, the resultant beam may be plane or circularly polarized.

Case 1. $\delta = n\lambda$, $n = 0, 1, 2$, etc. Equation [2] becomes

$$\frac{x}{a} - \frac{y}{b} = 0.$$

The emergent light is plane-polarized, the vibrations being in the same direction as the original beam.

Case 2. $\delta = (2n + 1)\,\lambda/2$. Equation [2] reduces to

$$\frac{x}{a} + \frac{y}{b} = 0.$$

The emergent light is plane-polarized in a direction making an angle 2ϵ with the original beam.

Case 3. $\delta = (2n + 1)\,\lambda/4$, $\epsilon = 45°$. Equation [2] becomes

$$x^2 + y^2 = a^2.$$

The emergent beam is circularly polarized. For $\delta = \lambda/4$ the vibration corresponds to the motion of a particle moving in a clockwise direction; for $\delta = 3\lambda/4$ the circular vibration will be counter-clockwise.

Double Refraction of Circularly Polarized Light

Circularly polarized monochromatic light consists of two mutually perpendicular vibrations of equal amplitude and 90° out of phase. The vibrations can be represented by

$$\begin{aligned} x' &= a \cos 2\pi \frac{t}{T} \\ y' &= a \sin 2\pi \frac{t}{T} \end{aligned} \qquad [3]$$

On entering the crystal each of the beams will be broken up into two components, one parallel and the other perpendicular to the optic axis as shown in Figure 2. The components will be represented by

$$\begin{aligned} x &= a \cos \epsilon \cos 2\pi \frac{t}{T} - a \sin \epsilon \sin 2\pi \frac{t}{T} \\ &= a \cos \left(2\pi \frac{t}{T} + \epsilon\right) \\ &= a \cos 2\pi \frac{t'}{T} \end{aligned} \qquad [4]$$

and

$$\begin{aligned} y &= a \sin \epsilon \cos 2\pi \frac{t}{T} + a \cos \epsilon \sin 2\pi \frac{t}{T} \\ &= a \sin \left(2\pi \frac{t}{T} + \epsilon\right) \\ &= a \sin 2\pi \frac{t'}{T} \end{aligned} \qquad [5]$$

It is seen that regardless of the orientation of the optic axes of the crystal, circularly polarized light will yield two components of equal amplitude, one parallel and the other perpendicular to the optic axis and 90° out of

phase. Again since the velocity is different along the two axes, a path difference δ will result from the two components passing through the crystal. After combining these components and eliminating t, the resultant vibration is given by

$$x^2 + y^2 - 2xy \sin 2\pi \frac{\delta}{\lambda} = a^2 \cos^2 2\pi \frac{\delta}{\lambda} \qquad [6]$$

The emergent beam is elliptically polarized due to phase change between the components.

Measurement of Double Refraction

Double refraction is most simply measured in terms of the light path difference δ which is given in terms of the wavelength,

$$\delta = N\lambda \qquad [7]$$

where N is the fringe order. For example, if the crystal were of the right thickness so as to cause a path difference of one wavelength, a plane or circularly polarized monochromatic beam would emerge unchanged; the fringe order would be unity. If the plane-polarized light were passed through an analyzer with its optic axis set perpendicular to the axis of the polarizer, the beam would be extinguished. Similarly, any integral fringe order (N = 0, 1, 2, ...) will show as a dark field.

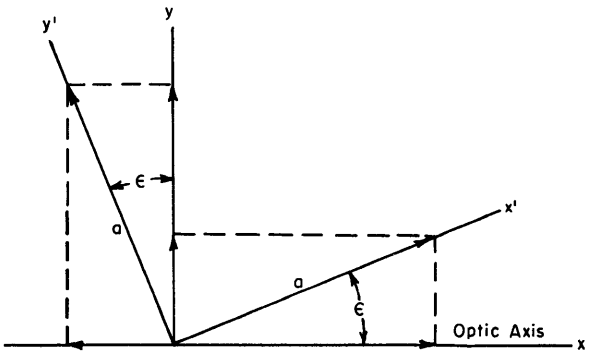

Figure 2 - Sketch Showing Components of Circularly Polarized Beam

Circularly polarized monochromatic light can be used in an analogous fashion to determine the fringe order, but the analysis is slightly more complicated. Circularly polarized light is produced by passing monochromatic plane-polarized light with a known direction of vibration through a quarter-wave plate, which is a crystal whose optic axis makes an angle of 45° with the plane of vibration of the polarized light and whose thickness is just sufficient to cause a retardation of $\lambda/4$ for the given wavelength. Then from Equation [2], the emergent light is circularly polarized. If a second quarter-wave plate is inserted whose axis makes an angle of 90° with the first quarter-wave plate, the result is a plane-polarized light whose vibrations are parallel to the original vibrations from the polarizer. If, now, the

analyzer has its optic axis set at 90° to that of the polarizer, the beam will be extinguished as it would for a plane-polarized beam with no quarter-wave plates.

The crystal to be studied is inserted in the beam of circularly polarized light between the two quarter-wave plates, as shown in Figure 3. If the thickness of the crystal is such that a retardation $\delta = N\lambda$ results, no change occurs in the emerging beam and the field remains dark. If the crystal produces a retardation $\delta = \frac{(2n + 1)}{2} \lambda$, the emergent beam will be circularly polarized but in the opposite direction of rotation. Thus the beam which passes through the second quarter-wave plate will be plane polarized at right angles to the original plane of polarization and the field as viewed through the analyzer will be bright. If, however, the crystal produces an arbitrary retardation, the emerging beam will be elliptically polarized. The second quarter-wave plate will produce two plane-polarized beams, one parallel and the other perpendicular to the axis of the polarizer. Thus, one of these beams will pass through the analyzer. Therefore, use of monochromatic circularly polarized light with a crossed setup as shown in Figure 3 would result in dark fringes only when $\delta = N\lambda$, just as for monochromatic plane-polarized light.

PHOTOELASTIC APPLICATION

When a transparent specimen is stressed, the particles become temporarily double refracting.[20] If monochromatic polarized light is passed through the specimen and the emergent beam studied by means of the analyzer, it is found that the field appears as a series of light and dark bands. It has been experimentally shown that the fundamental relationship between the stress at any point and the birefringence is given by

$$N = F \tau_{max} l \qquad [8]$$

where τ_{max} is the maximum shear stress, F is a constant for the particular material used known as the optical constant and l is the thickness of the specimen. The optical constant is determined by calibration, and once the fringe order is obtained, the shear stress throughout the field can be evaluated.

If monochromatic plane-polarized light is used in photoelastic studies, then examination of Equation [2] shows that there would be no change in the plane of polarization under two conditions:

$$1.\quad \delta = N\lambda \qquad N = 0,\ 1,\ 2,\ \cdots \qquad [9]$$

$$2.\quad \epsilon = 0,\ \frac{\pi}{2} \quad (a \text{ or } b = 0) \qquad [10]$$

The second condition signifies that the optic axis of the specimen lies in the plane or perpendicular to the plane of vibration of the polarized light. Therefore, if plane-polarized light were used in studying a stress system, not only would dark fringes appear wherever N was an integer but also wherever the optic axis of the crystal lay in a plane parallel to or normal to the plane of polarization. For this reason, plane-polarized light is not used to obtain the stress distribution.

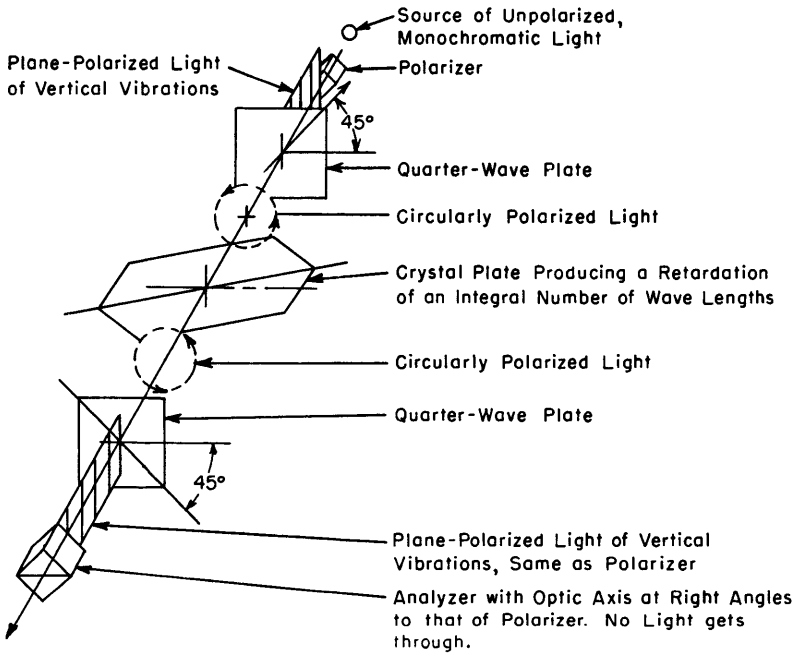

Figure 3 - Schematic Diagram Showing Extinction of Circularly Polarized Light when $\delta = N\lambda$

With monochromatic circularly polarized light, dark fringes occur only when $\delta = N\lambda$ and the order of the fringe is easily obtained by counting from the zero fringe. If the zero fringe is not readily obtainable from the configuration, it may always be found by the use of white light. In white light only the zero fringe is dark; the others are colored.

A similar technique may be used to determine the stress pattern in a hydrodynamic system. However, it must be demonstrated that Equation [8] is applicable. Whereas the optical constant in a photoelastic system is a constant, its equivalent S in a hydrodynamic system may be a function of the shearing rate.[21,22,23]

RECOMMENDED OPTICAL INSTALLATION

A recommended optical installation for photographing the stress pattern set up in hydrodynamic flow is shown in Figure 4. The bentonite channel is set between the polarizer and analyzer, each of which consists of a large polaroid screen and quarter-wave plate. The optic axis of the analyzer is set perpendicular to the axis of the polarizer so that the zero fringe is dark. Two large lenses are needed, one to insure parallel rays through the test section and the other to refocus the light. If sufficiently large lenses are not available suitable reflectors may be substituted.

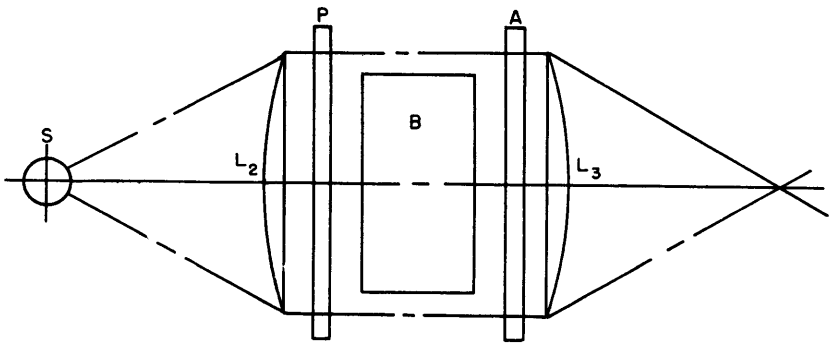

S is the light source, either white or monochromatic,

L_2,L_3 are the collimating lenses,

P is the polarizer with removable quarter-wave plate,

A is the analyzer with removable quarter-wave plate and with optic axis set at 90 degrees with that of polarizer, which makes the zero fringe the dark fringe, and

B is the bentonite channel test section or the light gap.

Figure 4 - Recommended Optical Setup

A good monochromatic light source is a mercury vapor lamp with a filter to absorb the violet line (No. 77 Wratten or a suitable Wainwright filter). This leaves a green line with a wavelength of 5.461×10^{-5} cm. A mica quarter-wave plate 0.03333 inch thick can be used to obtain circularly polarized light.

For small values of shear, retardation may be less than one wavelength so that only the zero fringe may appear. To measure path differences of less than a wavelength a Babinet-Soleil compensator[20,23] may be used. This is composed of two wedge-shaped crystals whose combined thickness can be varied. The elliptically polarized light emerging from the test specimen is passed through the compensator and the thickness of the crystal is adjusted by sliding one wedge over the other so that the total path difference is one wave-

length. This results in a dark fringe. The compensator is calibrated so that the path difference provided by the specimen can be read directly.

HYDRODYNAMIC STUDIES

Flowing colloidal solutions are doubly refracting in much the same way that stressed solid crystals are. Whether or not photoelastic methods can be extended into the realm of hydrodynamics must be determined by an analysis of the causes of double refraction in liquids. This analysis includes a study of the motion of colloidal particles under the influence of hydrodynamic forces. Methods of calibrating the flow against double refraction must be devised.

REVIEW OF LITERATURE

The phenomenon of streaming double refraction has been observed and measurements of the birefringence have been made as far back as 1870, but its complete explanation has been slow in development, and in particular, its application to flow studies has not been presented comprehensively.

Streaming Birefringence in Pure Liquids

Two theories have been presented for the cause of streaming double refraction in pure liquids. One theory assumes that the birefringence is caused by the deformation of ordinarily optically isotropic particles as in a photoelastic system while the other theory assumes that it is caused by the change in orientation of geometrically and optically anisotropic particles.

Kuhn[2] and Weller[23] apply the deformation theory to the case of pure liquids for which the analogy to a photoelastic system would be perfect. The optic axes of the fluid under stress due to flow would coincide with the principal stress planes and therefore make an angle of 45° with the plane of maximum shear, which they assumed would coincide with the streamline. Experimentally, they found that the birefringence was a function of the shear rate (velocity gradient). Weller found that for some liquids, the optic axes did not make an angle of 45° with the streamlines and concluded that the optic axes of these liquids did not coincide with the principal stress planes.

G.I. Taylor[24] performed some experiments with emulsions which showed that a particle of the emulsified liquid would tend to deform by lengthening along the principal plane for tension and shortening along the principal plane for compression.

Raman and Krishnan[25] suggest a different explanation for the phenomenon of streaming double refraction in pure liquids. They discuss the motion of ellipsoidal particles of molecular size. Using the method of Stokes, inertia forces are neglected and shear stresses are replaced by mutually perpendicular tension and compression stresses at an angle of 45° to the maximum shear stress plane. It was also assumed that the particles tended to orient themselves with their long dimensions along the principal stress plane for tension. The Brownian movement which is a random motion of the molecules due to their thermal agitation tends to disorient the array. Since the motion is studied at a point, only the rotary effect of the Brownian movement is of concern and must be considered as rotary motion in either direction. The resultant average equilibrium position can be determined statistically. The analysis leads to the conclusion that the average equilibrium position is such that the long axis of the ellipsoid lies in the plane of pure tension and the short axis lies in the plane of pure compression. This preferred orientation of geometrically and optically anisotropic particles causes double refraction. The number of particles oriented in this position at any instant in a given liquid is dependent upon the magnitude of the shear. In addition, the optic axis of the particle was assumed parallel to the long axis of the ellipsoid. This would mean that the optic axis makes an angle of 45° with the plane of maximum shear and that the birefringence is directly proportional to the shear. This method yields results very similar to the analyses of Kuhn and Weller except that orientation rather than deformation was assumed to cause double refraction in pure liquids.

Streaming Birefringence in Colloidal Solutions

The results of various experiments indicate that the problem is far more complex for particles of colloidal size.[22,26] It was found that birefringence was due mainly to the orientation of the particles which were usually long rods or flat plates. An accurate analysis of the motion of colloidal particles in a viscous incompressible fluid is extremely difficult because of the complexity of the hydrodynamic equations involved and because of the added complication of Brownian movement which, for colloidal particles, is due to the bombardment of the particles by the molecules of the surrounding medium. Jeffery[27] obtained the equations of motion for small ellipsoidal particles in which Brownian movement was neglected. He could not solve the general equations except for one specific case where the flow was given by:

$$u = cy$$
$$v = 0 \qquad [11]$$
$$w = 0$$

For this condition of flow, a slender rod would align itself in any direction in a plane of constant velocity while a disk would take any position in which its faces are parallel to streamlines.

Burgers[28] extended Jeffery's analysis for the same flow condition and showed that these slender particles would spend more time with their axes parallel to the direction of motion of the liquid. Boeder[29] investigated the effect of Brownian movement. Just as Jeffery and Burgers did, he used the flow represented by Equation [11] and showed that the extinction angle (the angle between the optic axis of the particle and the streamline) and the birefringence were functions of the intensity of Brownian movement and the velocity gradient. For low velocity gradients, the extinction angle is 45° and decreases with increasing velocity gradient. The extinction angle decreases but slightly with increasing velocity gradient when there is vigorous Brownian movement while it approaches zero when the Brownian movement is of small intensity. This agrees very well with experimental results.

Langmuir[30] sought to account for the variation in the extinction angle by assuming the presence of long range forces acting between the particles with a resultant tilting. This hypothesis does not seem very satisfactory because, in dilute solutions, the distances through which these intermolecular forces must act would be relatively tremendous.[31]

Almost everyone using double refraction methods adopted Boeder's conclusions and assumed that the orientation of a particle with respect to the streamline and the birefringence were both proportional to the velocity gradient.

Calibration Equipment and Equations

Apparatus for determining the relationship between birefringence and velocity gradient and also between the extinction angle and the velocity gradient was almost invariably the concentric-cylinder type (Kundt cell) with either the inner or outer cylinder rotating. In spite of its long use, a number of different expressions have been used to relate the various parameters measured by the Kundt cell. Most experimenters used a narrow gap and assumed the cylinders could be treated as two parallel plates.[32,33] The resultant expressions for the case when the inner cylinder is rotating are

$$\frac{N}{l} = \mu M \frac{dV}{dn} \qquad [12]$$

and

$$\frac{dV}{dn} = \frac{\omega r_i}{r_o - r_i} \qquad [13]$$

where M is an optical constant known as the Maxwell constant.

Sadron,[4,34] although he used the above relationships in his analysis, suggested improvements of the following form:

$$\frac{N}{l} = \mu M \left(\frac{\partial V}{\partial n} - \frac{V}{\rho}\right) \qquad [14]$$

and

$$V = \frac{\omega r\left(\frac{1}{r^2} - \frac{1}{r_0^2}\right)}{\frac{1}{r_i^2} - \frac{1}{r_0^2}} \qquad [15]$$

Equation [14] corrects for curvilinear motion while Equation [15] is a more accurate representation of the velocity distribution between rotating cylinders.

The narrow gap used in all the previous references introduced errors caused by depolarization and reflection from the walls of the cylinder. A wider gap would be preferable. Weller,[23] in his studies, used a comparatively wide gap of 0.516 cm and used the following relationships:

$$\frac{N}{l} = \mu M \frac{dV}{dn} \qquad [16]$$

and

$$\frac{dV}{dn} = \frac{r_i \omega}{r \ln \frac{r_o}{r_i}} \qquad [17]$$

Robinson[18] used a gap 1.135 cm. wide and determined the birefringence at various points across the annulus.

Birefringence Calibration

The technique of birefringence calibration is fairly well standardized. With the dimensions of the Kundt cell known and a set of relationships for birefringence and velocity gradient as a function of the angular velocity selected, the Maxwell constant can be determined. For a given angular velocity, the velocity gradient is known. The viscosity μ, can be obtained by using the Kundt cell as a rotary viscometer, that is by determining the torque

necessary to maintain the prescribed angular velocity and comparing it with that required for liquids of known viscosity. The birefringence is determined optically by use of circularly polarized light. A plot of $N/\mu l$ against dV/dn can be made. If the graph is a straight line, the Maxwell constant M is truly a constant and is given by the slope. Otherwise the value of M corresponding to any point is the ratio of $N/\mu l$ to dV/dn for that point.

Measurement of Extinction Angle

The extinction angle χ is defined as the angle between the optic axis of the birefringent particle and the streamline. In photoelastic specimens, it has been found that the optic axis coincides with the principal tension plane[20] but this is not true in colloidal solutions. The Kundt cell may be used very readily to determine χ. The simplest method is to view one point in the field of the Kundt cell with plane-polarized light and to rotate the plane of polarization until extinction occurs as shown in Figure 5. The plane of polarization then coincides with the optic axis[35,36] and the angle between this plane and the streamline is χ.

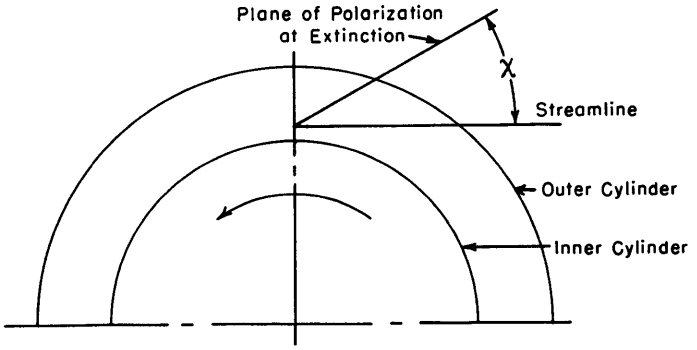

Figure 5 - Sketch Showing Method of Determining χ

Application of the Phenomenon of Streaming Birefringence to Flow Studies

Sadron,[4,34] Weller,[23] and Dewey[6,37] constructed channels for studying fluid flow. Sadron used a pure liquid, sesame oil, in two different sections, one parallel, the other diverging and determined the velocity distribution by means of Equation [12]. Weller studied the flow around different bodies in a test section using a solution of ethyl cellulose. He obtained the velocity distribution for a parallel channel and suggested a method for obtaining it for more general cases. However, his equations are not explicit enough to indicate the method of integration.

Dewey employed a colloidal solution of bentonite and made a considerable survey using a number of different models. He assumed that there was, under all circumstances, a definite relationship between the birefringence and the velocity gradient and also between the extinction angle and the velocity gradient. He determined these relationships by calibration of a Kundt cell. For a 1.25 percent solution of bentonite in water, the extinction angle decreased with increasing velocity gradient, asymptotically approaching about 12 degrees. The birefringence increased nonlinearity with velocity gradient. By photographing the stress pattern for the complete field, he obtained the velocity gradient at each point in the field and from this inferred the extinction angle. In addition he obtained the isoclinic curves and finally the streamlines about different models.

In photoelasticity, an isocline is the locus of points at which the principal stress planes and hence the optic axes make constant angles with a fixed reference plane. Isoclinic curves may be similarly determined in streaming birefringence. For any two particles to have the same isocline, they must be oriented in the same direction. Therefore, at any specified isocline ζ, all particles along the isocline have the same orientation and the optic axes make the same angle ζ with the reference plane. The reference plane is taken as the horizontal plane which is most convenient for the computations involved. An isoclinic curve can be obtained for any specified plane of polarization (ζ = 5°, 10°, 15°, etc.) by sketching in that portion of the dark fringe obtained by using plane-polarized white light which does not appear when circularly polarized light is used. From Equation [10] this portion of the zero fringe delineates regions in which the optic axis has the specified direction.

Once the extinction and the isoclinic angles are known at any point, the orientation of the streamline β can be determined. From Figure 6 it is evident that

$$\beta = \chi + \zeta \qquad [18]$$

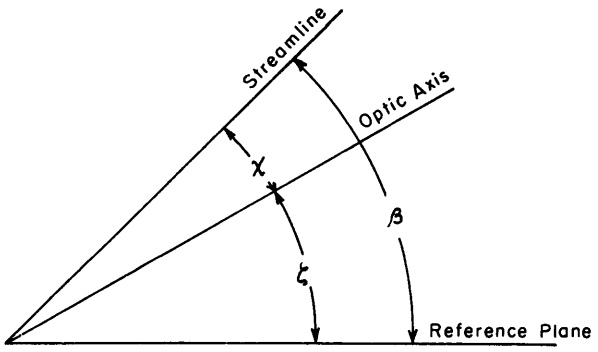

Figure 6 - Sketch Showing Orientation of Streamline

Dewey used a similar technique to obtain the streamlines around a number of forms.

PROPOSED APPLICATION OF PREVIOUS DEVELOPMENTS TO BENTONITE SOLUTIONS

The work of Sadron, Boeder, and others are consistent with the following set of assumptions concerning flowing colloidal solutions of bentonite:

1. Hydrodynamic forces tend to orient the particles, which are flat, plate-like crystals, so that the plane of the particle is in the streamline.

2. Brownian movement tends to disrupt this orientation; as a result the equilibrium position is a statistical problem.

3. The birefringence is a function of the velocity gradient, not necessarily linear, which may be represented by the equation:

$$\frac{N}{l} = f\left(\frac{\partial V}{\partial n} - \frac{V}{\rho}\right) \qquad [19]$$

Utilizing the above assumptions, the velocity distribution of a model in the test section may be determined.

The Test Facility

For the purpose of studying flow phenomena by means of bentonite solutions, a facility is now under construction at the David Taylor Model Basin. The general layout is shown in Figure 7.

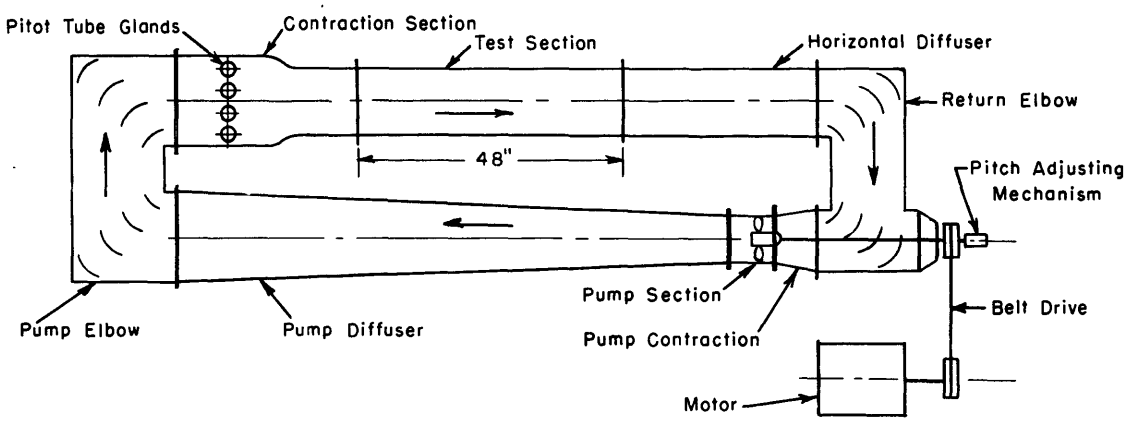

Figure 7 - Sketch Showing Major Features of the Bentonite Channel

A variable-pitch impeller will drive the bentonite solution around a closed channel at speeds up to 20 feet per second in the test section, which is designed for two-dimensional studies at present. The test section is 48 inches long, 12 inches high, and 1 inch wide, being confined between two parallel glass plates which have been specially treated to remove residual stresses. These dimensions were selected in order to obtain two-dimensional flow

with sufficient length and depth to approximate infinite boundaries. Plastic models will be held in the test section and the flow around them will be analyzed.

The contraction section leading up to the test section has been designed with a special set of glands for use as a pitot probe installation. Thus the discharge through the test section can be obtained for any particular pump speed and setting.

Determination of Velocity Distribution

The extinction angle and $\partial V/\partial n - V/\rho$ can be calibrated against N/l by means of the Kundt cell as described in an earlier section. A photograph of the stress pattern will give N/l throughout the field; therefore, the extinction angle and $\partial V/\partial n - V/\rho$ are known throughout the field. Isoclinic curves, giving the orientation of the optic axis, combined with the extinction angle give the direction of the streamlines throughout the field. Once the directions are known the actual streamlines can be mapped. Figure 8 represents such a mapping.

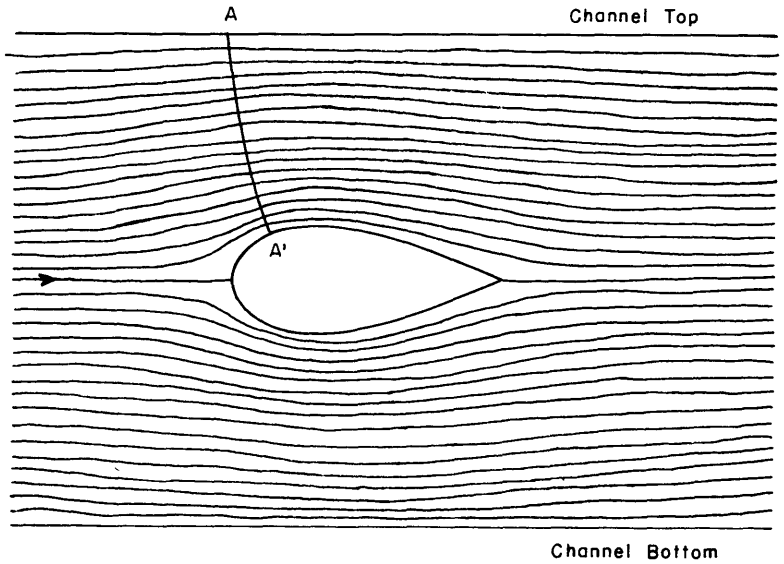

Figure 8 - Typical Mapping of Streamlines
Used to Obtain Velocity Distribution

Once the streamlines are constructed, the normal lines such as A-A' can be drawn. Since $\partial V/\partial n - V/\rho$ is known throughout the field we may write

$$\frac{\partial V}{\partial n} = f(x,y) + \frac{V}{\rho} \qquad [20]$$

Integrating along a normal line such as A-A' the partial derivative may be replaced by the ordinary derivative; f(x,y) is known and ρ can be determined graphically. This form of differential equation can be integrated by numerical methods but the method is tedious and too exact for the accuracy of the measurements. Instead the difference equation* may be written

$$\frac{\Delta V}{\Delta n} = \frac{V_{n+1} - V_n}{\Delta n} = \frac{V_n}{\rho_n} + f(x,y) \qquad [21]$$

At the boundary n = 0 and $V_n = 0$. Then

$$V_1 = \Delta n \; f(x,y) \qquad [22]$$

This procedure can be extended along A-A', the size of the increments determining the accuracy of the calculation.

FURTHER INVESTIGATION INTO THE HYDRODYNAMICS OF COLLOIDAL PARTICLES

One of the assumptions in previous work which may be open to question is the one assuming that the bentonite particles orient themselves in the plane of the streamline as a consequence of the hydrodynamic forces on them. The analyses of Burgers, Jeffery, and Boeder, although indicating this to be so, lacked generality because of the very restricted flow condition considered. Therefore, the following analysis was made for the more general case of two-dimensional flow.

Equilibrium Position of Very Slender Colloidal Particles in Two-Dimensional Flow, Neglecting Brownian Movement

It will be assumed that the birefringent particles are very slender particles of length $2l$ which are so small that inertia forces on them may be neglected, and their motion is the same as the motion of the fluid immediately surrounding them. The orientation of any particle may then be represented as a radius vector OP = l in a set of axes moving with the particle. Let the origin of the axes coincide with the center of mass of the particle and let its orientation be specified by the polar and azimuthal angles θ and ϕ respectively; see Figure 9. For two-dimensional flow, in a plane normal to the Z axis, the velocity components of the point P, the end of the particle, may be represented by the two components parallel to the x and y axes, u_p and v_p. These components may be resolved into two mutually perpendicular components; u_ϕ perpendicular to the meridian plane ZOP tending to alter ϕ and u_θ in the

*V_n is not the normal component of the velocity which is always zero but the velocity at a distance n from the boundary measured along A-A'.

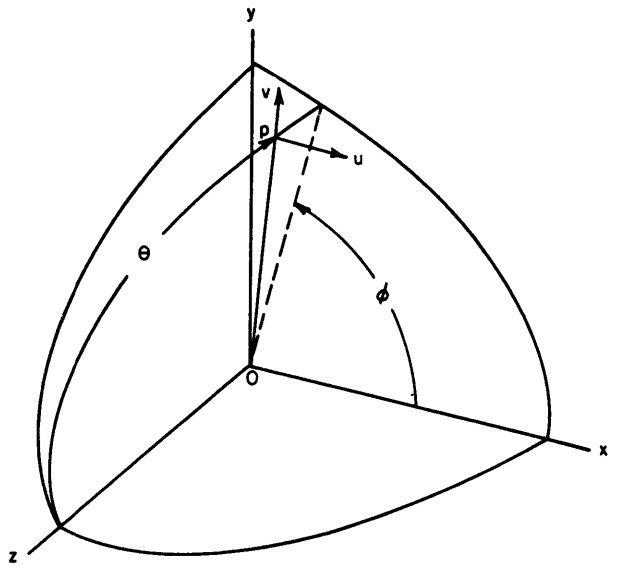

Figure 9 - Sketch Showing Variables Used in Determining Equilibrium Position

meridian plane tending to alter θ. As the particle is assumed to be rigid there will be no motion along the length of the particle.

The values of u_ϕ and u_θ in terms of u_P, v_P are:

$$u_\phi = l \sin\theta \dot{\phi} = -u_P \sin\phi + v_P \cos\phi \qquad [23]$$

$$u_\theta = l \dot{\theta} = u_P \cos\theta \cos\phi + v_P \cos\theta \sin\phi \qquad [24]$$

The values of u_P and v_P relative to 0 which is moving with the particle are:

$$\left.\begin{aligned} u_P &= \frac{\partial u}{\partial y} l \sin\theta \sin\phi + \frac{\partial u}{\partial x} l \sin\theta \cos\phi \\ v_P &= \frac{\partial v}{\partial y} l \sin\theta \sin\phi + \frac{\partial v}{\partial x} l \sin\theta \cos\phi \end{aligned}\right\} \qquad [25]$$

Substituting Equations [25] in [23]

$$\begin{aligned} l \sin\theta \dot{\phi} = -\Big[&\frac{\partial u}{\partial y} l \sin\theta \sin^2\phi + \frac{\partial u}{\partial x} l \sin\theta \sin\phi \cos\phi\Big] \\ &+ \frac{\partial v}{\partial y} l \sin\theta \sin\phi \cos\phi + \frac{\partial v}{\partial x} l \sin\theta \cos^2\phi \end{aligned} \qquad [26]$$

or

$$\dot{\phi} = \frac{\partial u}{\partial y} \sin^2\phi - \left(\frac{\partial u}{\partial x} - \frac{\partial v}{\partial y}\right) \sin\phi \cos\phi + \frac{\partial v}{\partial x} \cos^2\phi \qquad [27]$$

This equation can be simplified by a rotation of the x and y axes into the planes of maximum shear. For convenience, it is assumed that enough is known about the flow so that the axes may be chosen in such a manner that the streamline is in the first quadrant with the direction of flow in the positive x direction.

Then

$$\frac{\partial u}{\partial x} = \frac{\partial v}{\partial y} = 0 \qquad [28]$$

and from Equation [27]

$$\dot{\phi} = \frac{\partial v}{\partial x} \cos^2 \phi - \frac{\partial u}{\partial y} \sin^2 \phi \qquad [29]$$

Since the particle is moving with the streamline, solutions to Equation [29] are needed in which $\dot{\phi} = \dot{\alpha}$ (the rate of turning of the tangent to the streamline). Particles so oriented will maintain a constant angle to the streamline. The relation between α and the velocity components is shown in Figure 10. Now

$$\dot{\alpha} = \frac{V}{\rho} = \frac{V \dfrac{d^2y}{dx^2}}{\left[1 + \left(\dfrac{dy}{dx}\right)^2\right]^{3/2}} \qquad [30]$$

where

$$\frac{dy}{dx} = \frac{v}{u} \qquad [31]$$

and

$$\frac{d^2y}{dx^2} = \frac{u \dfrac{dv}{dx} - v \dfrac{du}{dx}}{u^2} \qquad [32]$$

Using Equation [28]

$$\frac{dv}{dx} = \frac{\partial v}{\partial x} + \frac{\partial v}{\partial y} \frac{dy}{dx} = \frac{\partial v}{\partial x} \qquad [33]$$

also

$$\frac{du}{dx} = \frac{\partial u}{\partial x} + \frac{\partial u}{\partial y} \frac{dy}{dx} = \frac{\partial u}{\partial y} \frac{v}{u} \qquad [34]$$

Substituting these values in Equation [32] gives

$$\frac{d^2y}{dx^2} = \frac{1}{u^2} \left(u \frac{\partial v}{\partial x} - \frac{v^2}{u} \frac{\partial u}{\partial y}\right) \qquad [35]$$

Substituting for dy/dx and d^2y/dx^2 in Equation [30] and recalling that $u^2 + v^2 = V^2$, it follows that

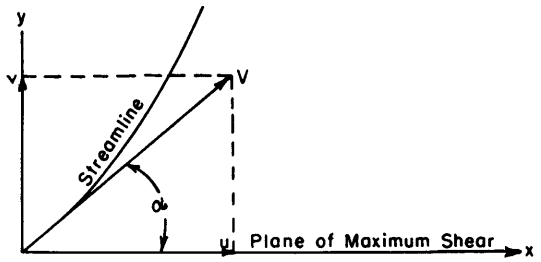

Figure 10 - Sketch Showing Terms Used in Equations [30] and [31]

$$\dot{\alpha} = \frac{1}{V^2}\left(u^2\frac{\partial v}{\partial x} - v^2\frac{\partial u}{\partial y}\right) = \frac{\partial v}{\partial x}\cos^2\alpha - \frac{\partial u}{\partial y}\sin^2\alpha \qquad [36]$$

Solutions of ϕ in [29] are needed in which $\dot{\phi} = \dot{\alpha}$. Combining Equations [29] and [36] gives

$$\frac{\partial v}{\partial x}\cos^2\phi - \frac{\partial u}{\partial y}\sin^2\phi = \frac{\partial v}{\partial x}\cos^2\alpha - \frac{\partial u}{\partial y}\sin^2\alpha \qquad [37]$$

Therefore

$$\frac{\partial v}{\partial x}(\cos^2\phi - \cos^2\alpha) - \frac{\partial u}{\partial y}(\sin^2\phi - \sin^2\alpha) = 0 \qquad [38]$$

But

$$\cos^2\phi - \cos^2\alpha = -\sin^2\phi + \sin^2\alpha \qquad [39]$$

Consequently

$$\left(\frac{\partial v}{\partial x} + \frac{\partial u}{\partial y}\right)(\sin^2\phi - \sin^2\alpha) = 0 \qquad [40]$$

If $\partial v/\partial x + \partial u/\partial y = 0$, ϕ may have any value. But this condition means pure rotation only. Otherwise

$$\sin^2\phi = \sin^2\alpha$$
$$\phi = \pm\alpha,\ \pi \pm \alpha \qquad [41]$$

However, adding π makes no difference for these particles.

Significance of Solutions for ϕ

Equation [41] indicates that there are two solutions for ϕ which satisfy Equation [37]. In one of these the particle lies in the streamline; in the other, the particle makes the same angle with the plane of maximum shear as does the streamline but lies on the opposite side of the plane of maximum shear.

It would be desirable to ascertain the conditions under which each would be the stable position. Two cases occur according as the value $\phi = 0$ makes $\dot{\phi}$ either a minimum or maximum.

Case I. $\dot{\phi}$ is a maximum at $\phi = 0$. This occurs when

$$\frac{\partial v}{\partial x} + \frac{\partial u}{\partial y} > 0 \qquad [42]$$

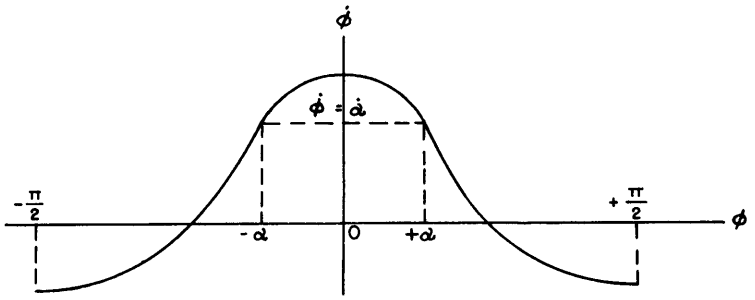

Figure 11 - Variation of $\dot{\phi}$ with ϕ for Case I $\left(\frac{\partial v}{\partial x} + \frac{\partial u}{\partial y} > 0\right)$

Figure 11 shows the relation between $\dot{\phi}$ and ϕ for this condition. When $\phi = \pm \alpha$, $\dot{\phi} = \dot{\alpha}$. Examination of the curve of Figure 11 shows that for $|\phi| < |\alpha|$, $\dot{\phi} > \dot{\alpha}$. Therefore ϕ will increase toward α and the particle will turn into the streamline. For $|\phi| > |\alpha|$, $\dot{\phi} < \dot{\alpha}$ and the particle will also turn into the streamline.

Case II. $\dot{\phi}$ is a minimum when $\phi = 0$. For this case it is necessary that

$$\frac{\partial v}{\partial x} + \frac{\partial u}{\partial y} < 0 \qquad [43]$$

The variation of $\dot{\phi}$ with ϕ for this case is shown in Figure 12. The curve shows that for $|\phi| < |\alpha|$, $\dot{\phi} < \dot{\alpha}$ and the particle will turn away from the streamline into the $-\alpha$ position. For $|\phi| > |\alpha|$, $\dot{\phi} > \dot{\alpha}$ and the particle will also turn away from the streamline into the $-\alpha$ position.

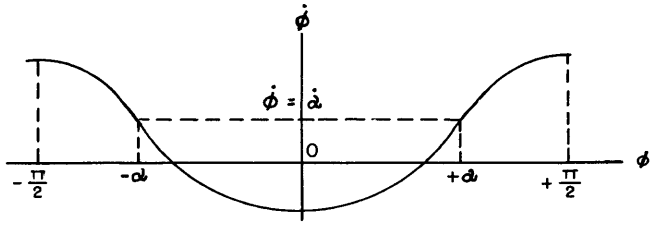

Figure 12 - Variation of $\dot{\phi}$ with ϕ for Case II $\left(\frac{\partial v}{\partial x} + \frac{\partial u}{\partial y} < 0\right)$

The actual flow conditions which will bring about either case can be readily ascertained. We can write

$$\frac{\partial V}{\partial s} = \frac{\partial V}{\partial x}\frac{\partial x}{\partial s} + \frac{\partial V}{\partial y}\frac{\partial y}{\partial s} = \frac{\partial V}{\partial x}\cos\alpha + \frac{\partial V}{\partial y}\sin\alpha \qquad [44]$$

Since $\partial u/\partial x = \partial v/\partial y = 0$ by virtue of the orientation of the axes, and

$$V = \sqrt{u^2 + v^2}$$

we obtain

$$\frac{\partial y}{\partial x} = \frac{v}{V}\frac{\partial v}{\partial x} = \sin \alpha \frac{\partial v}{\partial x} \qquad [45]$$

and

$$\frac{\partial V}{\partial y} = \frac{u}{V}\frac{\partial u}{\partial y} = \cos \alpha \frac{\partial u}{\partial y} \qquad [46]$$

Substituting from Equations [45] and [46] into Equation [44]

$$\frac{\partial V}{\partial s} = \sin \alpha \cos \alpha \frac{\partial v}{\partial x} + \sin \alpha \cos \alpha \frac{\partial u}{\partial y} = \frac{\sin 2\alpha}{2}\left(\frac{\partial v}{\partial x} + \frac{\partial u}{\partial x}\right) \qquad [47]$$

Here α can vary from 0 to $\frac{\pi}{2}$. In the trivial case $\alpha = 0$ or $\pi/2$, $\partial V/\partial s = 0$ and the flow is parallel. For $0 < \alpha < \pi/2$ when $\partial v/\partial x + \partial u/\partial y > 0$, $\partial V/\partial s > 0$. Thus, there is a positive velocity gradient, characteristic of convergent flow, and the particle would tend to turn into the flow. When $\partial v/\partial x + \partial u/\partial y < 0$, on the other hand, $\partial V/\partial s < 0$, the flow is divergent and the particle would turn away from the streamline.

STUDY OF THE EQUATION FOR $\dot{\theta}$

The corresponding equation for $\dot{\theta}$ may be obtained by substituting Equations [25] in [24]. Using condition [28], in which the streamlines are in the positive x direction, the expression for $\dot{\theta}$ becomes

$$\begin{aligned}\dot{\theta} &= \left(\frac{\partial u}{\partial y} + \frac{\partial v}{\partial x}\right) \sin \theta \cos \theta \sin \phi \cos \phi \\ &= \left(\frac{\partial u}{\partial y} + \frac{\partial v}{\partial x}\right) \frac{\sin 2\theta \sin 2\phi}{4}\end{aligned} \qquad [48]$$

For $\partial u/\partial y + \partial v/\partial x > 0$, the stable value of ϕ is $\phi = \alpha$ and, since θ varies only from 0 to $\pi/2$, $\dot{\theta}$ is positive; thus θ will increase until it equals $\pi/2$ and the axis of the particle is in the plane of motion. For $\partial u/\partial y + \partial v/\partial x < 0$, $\phi = -\alpha$ is the stable position and again $\dot{\theta}$ is positive and θ is stable at $\pi/2$. Thus it may be concluded that the particles will turn into a plane parallel to the planes of flow.

Extension to Bentonite Particles

Bentonite particles are plates, not rods. Assuming that a flat narrow plate follows as closely as possible the motion of the fluid particles, it should align itself with its long dimension in the position assumed by a rod and with its transverse dimension either in the plane of motion or perpendicular to it. In either case, the optic axis should have the same position

as for a rod which is along its axis.

Relation between Streamline and Plane of Maximum Shear

Since the analysis as developed indicates two possible positions for the particle, both related to the plane of maximum shear and the streamline, the relationship between these two would be important.

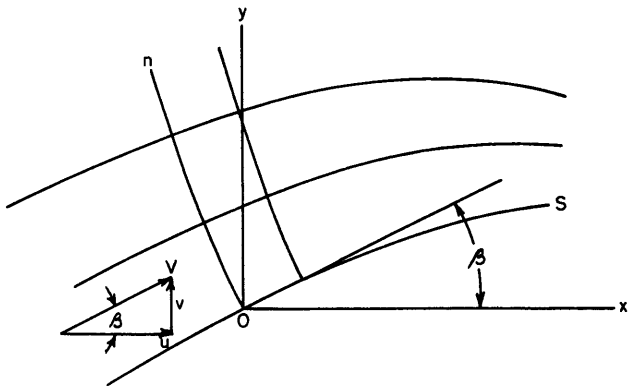

Figure 13 - Sketch Showing Relationship between Rectangular and Streamline Coordinates

The general expression for the shear in rectangular coordinates[38] is given by

$$\tau_{yx} = \tau_{xy} = \mu\left(\frac{\partial u}{\partial y} + \frac{\partial v}{\partial x}\right) \qquad [49]$$

Since only flow in the immediate neighborhood of a point is being considered, it will be convenient to use the stream coordinates s and n to define the motion. The coordinate s is along the streamline and n normal to it, as shown in Figure 13. In terms of the flow velocity and direction cosines of the streamline through the point, the velocity components are $u = l_1 V$ and $v = l_2 V$, where the direction cosines are evaluated in Table I.

TABLE 1

Matrix Giving Values of Direction Cosines

	ds	dn
dx	$l_1 = \cos\beta$	$m_1 = -\sin\beta$
dy	$l_2 = \sin\beta$	$m_2 = \cos\beta$

Then

$$\frac{\partial u}{\partial y} = \frac{\partial}{\partial y}(l_1 V) = \frac{\partial}{\partial s}(l_1 V)\frac{\partial s}{\partial y} + \frac{\partial}{\partial n}(l_1 V)\frac{\partial n}{\partial y}$$

$$= l_2\left(V\frac{\partial l_1}{\partial s} + l_1\frac{\partial V}{\partial s}\right) + m_2\left(V\frac{\partial l_1}{\partial n} + l_1\frac{\partial V}{\partial n}\right) \qquad [50]$$

and

$$\frac{\partial v}{\partial x} = \frac{\partial}{\partial x}(l_2 V) = \frac{\partial}{\partial s}(l_2 V)\frac{\partial s}{\partial y} + \frac{\partial}{\partial n}(l_2 V)\frac{\partial n}{\partial x}$$

$$= l_1\left(V\frac{\partial l_2}{\partial s} + l_2\frac{\partial V}{\partial s}\right) + m_1\left(V\frac{\partial l_2}{\partial n} + l_2\frac{\partial V}{\partial n}\right) \qquad [51]$$

Substituting [50] and [51] in [49]

$$\frac{\tau_{xy}}{\mu} = l_2\left(V\frac{\partial l_1}{\partial s} + l_1\frac{\partial V}{\partial s}\right) + m_2\left(V\frac{\partial l_1}{\partial n} + l_1\frac{\partial V}{\partial n}\right)$$

$$+ l_1\left(V\frac{\partial l_2}{\partial s} + l_2\frac{\partial V}{\partial s}\right) + m_1\left(V\frac{\partial l_2}{\partial n} + l_2\frac{\partial V}{\partial n}\right)$$

$$\frac{\tau_{xy}}{\mu} = \frac{\partial V}{\partial s}(2 l_1 l_2) + \frac{\partial V}{\partial n}(l_1 m_2 + m_1 l_2)$$

$$+ V\left(l_2\frac{\partial l_1}{\partial s} + l_1\frac{\partial l_2}{\partial s} + m_2\frac{\partial l_1}{\partial n} + m_1\frac{\partial l_2}{\partial n}\right)$$

$$\frac{\tau_{xy}}{\mu} = \frac{\partial V}{\partial s}\sin 2\beta + \frac{\partial V}{\partial n}\cos 2\beta + V\left(\frac{\partial \beta}{\partial s}\cos 2\beta - \frac{\partial \beta}{\partial n}\sin 2\beta\right) \qquad [52]$$

From the equation of continuity

$$\frac{\partial V}{\partial s} + V\frac{\partial \beta}{\partial n} = 0 \qquad [53]$$

Also

$$\frac{\partial \beta}{\partial s} = -\frac{1}{\rho} \qquad [54]$$

where ρ is taken negative when the center of curvature is on the same side of the streamline as the positive direction of dn. Therefore

$$\frac{\tau_{xy}}{\mu} = \cos 2\beta\left(\frac{\partial V}{\partial n} - \frac{V}{\rho}\right) + 2\sin 2\beta\frac{\partial V}{\partial s} \qquad [55]$$

The value of β, which will make τ_{xy} a maximum and for which $\beta = \alpha$, is readily determined by differentiating Equation [55].

$$\frac{d\,\tau_{xy}}{\mu\, d\beta} = -2\sin 2\beta\left(\frac{\partial V}{\partial n} - \frac{V}{\rho}\right) + 4\cos 2\beta\frac{\partial V}{\partial s} = 0$$

or

$$\tan 2\beta = \tan 2\alpha = \frac{2\frac{\partial V}{\partial s}}{\frac{\partial V}{\partial n} - \frac{V}{\rho}} \qquad [56]$$

Except when $\alpha = 0$ the plane of maximum shear does not coincide with the streamline. In convergent flow when $\phi = \alpha$ the particles tend to orient themselves into the streamlines, but in divergent flow when $\phi = -\alpha$ the particles tend to orient themselves away from the streamlines. Thus, the use of colloidal solutions to determine streamlines may lead to erroneous results, particularly in regions where it would be difficult to evaluate the velocity gradient. Therefore, the applicability of colloidal solutions in determining streamlines must be investigated experimentally. This cannot be done in rotating cylinders or any other parallel flow in which $\partial V/\partial s = 0$ because the plane of maximum shear coincides with a streamline, $\alpha = -\alpha = 0$. Tests will have to be made in a diverging channel in which the direction of the streamlines can be determined by other methods.

UTILIZATION OF DOUBLY REFRACTING PURE LIQUIDS FOR OBTAINING THE VELOCITY DISTRIBUTION

As an alternative to colloidal solutions, other experimenters have used pure liquids. Here the double refraction is due primarily to deformation rather than orientation of the molecules. Hence there would be a close analogy between the hydrodynamic and photoelastic system. The birefringence can be assumed to be a maximum along the plane of maximum shear and the magnitude of the maximum birefringence is proportional to the maximum shear.

Modification of Calibration Technique in Kundt Cell

In the Kundt cell, $\partial V/\partial s = 0$, hence the plane of maximum shear occurs along the streamline or normal to it and is equal to $\mu(\partial V/\partial n - V/\rho)$. Therefore, the Kundt cell can be used to calibrate τ_{max}/μ against N/l. In addition, since the direction of the plane of maximum shear is known and the orientation of the optic axis can be determined, the angle between these two as a function of N/l can be obtained. The most suitable equations[39,40] for V and dV/dn are given by

$$\frac{dV}{dn} = a - \frac{b}{r^2} \qquad [57]$$

and

$$V = ar + \frac{b}{r} \qquad [58]$$

where $a = \dfrac{-\omega r_i^2}{r_o^2 - r_i^2}$ and $b = \dfrac{\omega r_o^2 r_i^2}{r_o^2 - r_i^2}$

If the inner cylinder is stationary and the outer one rotates, r_o and r_i must be interchanged.

As there is some uncertainty in the applicability of some of the relations developed, it seems advisable to construct two Kerr cells with cylinders of different radii. In order to survey the birefringence at different points across the annulus, a movable slit may be placed between the light source and the Kerr cell. With the use of cylinders of different sizes and the movable slit, the effect of curvature and variation in velocity across the annulus may be determined.

Equations [57] and [58] are applicable only to laminar flow. The critical angular velocity for transition from laminar to turbulent flow in a Kerr cell with the inner cylinder rotating has been determined experimentally by G.I. Taylor[41] and is given by

$$\left(\frac{\omega}{\gamma}\right)^2 = \frac{\pi^4}{P} \frac{(r_i + r_o)}{(r_o - r_i)^3 \, r_i^2} \qquad [59]$$

where

$$P = 0.57 \left[1 - 0.652 \frac{r_o - r_i}{r_i}\right] + \frac{0.00056}{1 - 0.652 \dfrac{r_o - r_i}{r_i}}$$

Proposed Method of Determining Streamlines and Velocity Distribution from Stress Patterns

The following measurements must be made in order to obtain the streamlines and velocity distribution about a body in a channel:

1. The quantity of discharge, Q.
2. The stress pattern.
3. The isoclinic curves.

The quantity of discharge can be calibrated against pump speed and blade setting. The stress pattern is obtained by using circularly polarized light and photographing the resultant pattern. Also τ_{max}/μ has been calibrated against N/l by means of the Kundt cell. Therefore τ_{max}/μ can be determined for the complete field. The isoclinic curves which are obtained by using plane-polarized light are combined with the orientation of the optic axis with respect to the plane of maximum shear, as obtained in the Kundt cell, to give the orientation of the plane of maximum shear throughout the field.

Equations [55] and [56] do not lend themselves to any method of solution for determining the streamlines and the velocity distribution. Instead, knowing the magnitude and direction of the planes of maximum shear,

the magnitude of the horizontal shear at any point may be obtained by the relationship

$$\tau_{xy} = \tau_{max} \cos 2\eta \qquad [60]$$

where η is the angle from the horizontal to the plane of maximum shear. The horizontal and vertical components of the velocity may be expressed in terms of the stream function ψ

$$u = -\frac{\partial \psi}{\partial y} \qquad [61]$$

and

$$v = \frac{\partial \psi}{\partial x} \qquad [62]$$

Substituting for u and v in Equation [49] gives

$$\frac{\tau_{xy}}{\mu} = \frac{\partial^2 \psi}{\partial x^2} - \frac{\partial^2 \psi}{\partial y^2} \qquad [63]$$

This is a partial differential equation which can be solved by numerical methods if the boundary conditions are known.

Although a uniform velocity distribution in the test section of the channel is the goal, it cannot be achieved since the velocity is zero at the boundaries. However, well ahead of the model, the flow is essentially parallel which permits a ready determination of the velocity distribution. Let A-A' and B-B' in Figure 14 represent two planes normal to the flow in the region of parallel flow ($v \equiv 0$). The coordinate system has been selected so that A-A' and the channel bottom are the y- and x-axes respectively. The subscripts indicate the abscissae and ordinates respectively in terms of the step-lengths x_1 and y_1. For parallel flow ($v \equiv 0$), Equation [48] reduces to

$$\frac{\tau_{max}}{\mu} = \frac{\partial u}{\partial y} \qquad [64]$$

and u can be determined by numerical integration along lines A-A' and B-B'.

Once the velocity distribution is determined, the values of the stream function along the same lines can be obtained.

From Equation [61] for $v \equiv 0$,

$$d\psi = -u\, dy$$

or

$$\psi_{o,y} - \psi_{o,o} = -\int_0^y u\, dy \qquad [65]$$

$\psi_{o,o}$ can be set equal to zero. Then the value of the stream function at (o,y) is numerically equal to the area of the velocity distribution curve from y = 0 to y = y. In addition, the value of the stream function at the upper boundary ($\psi_{o,h}$) multiplied by the width of channel l should give the total discharge Q. Multiplying Equation [65] by l gives

$$\psi_{o,h}\ l = l \int_h^0 u\ dy = Q \qquad [66]$$

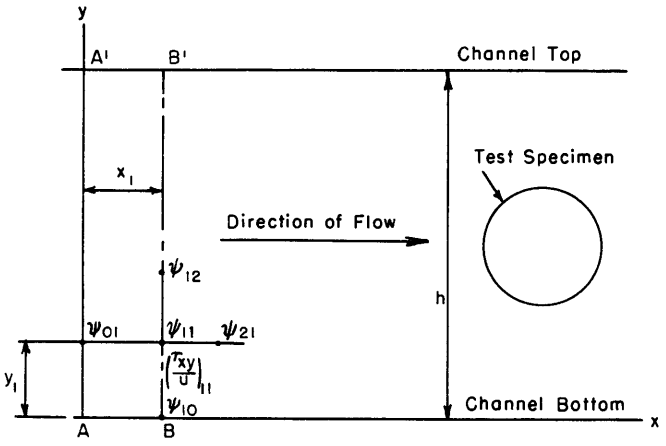

Figure 14 - Terms Used in Solution of Equation [63]

This method will give the values of the stream function ψ along the top and bottom boundaries and at all points sufficiently far from the model as not to disturb the flow, such as along A-A' and B-B'. Using A-A' and B-B' as two vertical elements of the grid, the results may be extrapolated to determine ψ throughout the field. This method is illustrated for determining ψ_{21}. The difference equations for $\partial^2\psi/\partial x^2$ and $\partial^2\psi/\partial y^2$ at x = 1, y = 1 are

$$\left(\frac{\partial^2\psi}{\partial x^2}\right)_{11} = \frac{\psi_{01} + \psi_{21} - 2\psi_{11}}{x_1^2} \qquad [67]$$

$$\left(\frac{\partial^2\psi}{\partial y^2}\right)_{11} = \frac{\psi_{10} + \psi_{12} - 2\psi_{11}}{y_1^2} \qquad [68]$$

Let $x_1 = y_1 = 1$ unit (0.1 foot, 0.01 foot etc. as desired). Substituting these values in Equation [63] gives

$$\left(\frac{\partial^2\psi}{\partial x^2}\right)_{11} - \left(\frac{\partial^2\psi}{\partial y^2}\right)_{11} = \left(\frac{\tau_{xy}}{\mu}\right)_{11} = \psi_{01} + \psi_{21} - \psi_{10} - \psi_{12}$$

or

$$\psi_{21} = \psi_{10} + \psi_{12} - \psi_{01} + \left(\frac{\tau_{xy}}{\mu}\right)_{11} \qquad [69]$$

Everything on the right hand side of Equation [69] is known. By continuing this extrapolation, the values of ψ throughout the field may be determined. Around the body the grid must be refined. Once ψ has been determined, u and v and their resultant V can be determined graphically. One check on the work is that ψ is a constant for any boundary. In addition, ψ can be determined for a normal line on the downstream side in the same way that A-A' was obtained. The values obtained for ψ by extrapolation can be further adjusted by some sort of relaxation method.

The accuracy of the method suggested for determining the velocity distribution is uncertain, since the errors are propagated by extrapolation. The refinement of technique necessary to get sufficiently accurate results may be extremely difficult, especially since some of the relationships depend upon statistical and hydrodynamic relationships which require verification.

DETERMINATION OF PRESSURE DISTRIBUTION

Once the streamlines and velocity distribution have been determined, the pressure distribution can be determined very readily by application of Bernoulli's equation for a streamline. Neglecting friction, this is

$$\frac{p_1}{\gamma} + \frac{V_1^2}{2} + gy_1 = \frac{p_2}{\gamma} + \frac{V_2^2}{2} + gy_2 \qquad [70]$$

p_1, V_1, and y_1 represent the upstream pressure, velocity and height of the streamline above the channel bottom, respectively, and p_2, V_2, and y_2 the same variables at a point further along the streamline where the pressure is desired. V_1 and V_2 have already been determined, p_1 is equal to the pressure at the top of the channel plus the gravity head and y_1 and y_2 can be measured directly. Therefore p_2 can be obtained. Since Equation [70] neglects friction, the error near the boundaries may be considerable.

DETERMINATION OF VISCOUS DRAG AND LIFT

Weller[23] discusses the utilization of streaming birefringence to determine viscous lift and drag. Figure 15 illustrates the technique for a disk, but the same method can be applied to various other forms.

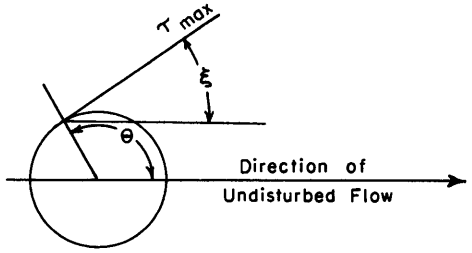

Figure 15 - Sketch Showing Drag Terms

For any surface element, the component of the shear parallel to the undisturbed direction of flow is $\tau_{max} \cos \xi$ since τ_{max} is tangent to the surface. The viscous drag is equal to the total shearing force in the direction of the resultant drag

$$D_v = \int_0^{2\pi} \tau_{max} \cos \xi \, d\theta \qquad [71]$$

where θ is the polar angle. The simplest method of solution would be to plot $\tau_{max} \cos \xi$ against θ and determine the area under the curve.

Similarly, the viscous lift can be obtained by taking the component normal to the flow and integrating around the body.

APPLICATION TO TURBULENT FLOW STUDIES

Very little has been done in the way of turbulent flow studies using the streaming birefringence methods and even that little is controversial. Weller[23] claimed that in his Kundt cell a dark band occurred in the center of the annulus at the onset of turbulence and that the birefringence outside of this band was not of the order anticipated. The appearance of the band was not in accord with the experiments of Sadron[34] who found that the equation relating birefringence and shear was satisfactory. However, extreme care had to be taken to use a point midway between the inner and outer cylinders.

Dewey[37] did a great deal of work on double refraction using bentonite solutions and took both still and motion pictures in turbulent flow. The onset of turbulence, turbulent eddies, and separation was clearly visible.

It is difficult to surmise whether mathematical relationships can be determined in order to relate shear and birefringence in turbulent flow. There should be some preferred orientation but the complex statistical nature of the motion may make it difficult to obtain useful quantitative relationships.

Besides the type of information obtained in Dewey's investigations, double refraction methods should be very useful in boundary layer studies for

both turbulent and laminary flow since both the thickness of and velocity distribution in the laminar boundary layer may be determined.

Whether rotating cylinders will be useful in determining the relationships between shear and birefringence in turbulent flow is problematical. There is some general information concerning the velocity distribution[42,43] between rotating cylinders. For most of the section, the velocity is found to follow the simple relationship

$$Vr = \text{constant} = C$$

or

$$\frac{dV}{dn} = -\frac{C}{r^2} \qquad [72]$$

where C is given by the theoretical equation

$$C = 0.5\ \omega\ r_i^2 \qquad [73]$$

Experiments by Taylor[41] indicate that the actual value of $Vr/\omega r_i^2$ varies from 0.504 to 0.541. Another difficulty is the nature of the flow in the Kundt cell. Some experiments have indicated the existence of vortices when the flow becomes turbulent which result in three-dimensional flow.[39,44]

THREE-DIMENSIONAL STUDIES

As yet little thought has been given to the application of streaming double refraction to three-dimensional flow studies. Methods using scattered light have been utilized in photoelasticity and may be applicable.[45] The California Institute of Technology has a three-dimensional test section which is used for qualitative studies.

CONCLUSIONS

An approximate analysis of the motion of a microscopic rod-like particle under the influence of hydrodynamic forces indicates that although bentonite solutions may be useful in studying the flow around two-dimensional bodies in the laminar region of flow, the relationships involving birefringence must be experimentally verified. A theoretical solution has been obtained by neglecting inertia forces and assuming the particle takes the motion of the surrounding medium without disturbing the flow. With this simplification it is found that for converging flow the long axis of the rod lies in the streamline; for diverging flow the equilibrium position of the long axis of the particle is not along the streamline but instead makes the same angle with

the plane of maximum shear as does the streamline but lies on the opposite side of the plane of maximum shear.

For test purposes, a 0.8 percent concentration with an e.s.d. of 50 mμ and an operating temperature of about 75° F. will be the most suitable bentonite solution as far as sensitivity, viscosity, and light transmission qualities are concerned.

Pure liquids can also be used for flow studies. Here, the analogy to a photoelastic system is closer and the analysis more straightforward. However, the sensitivity is much lower, and the viscosity much higher than bentonite solutions, both undesirable features.

Streaming birefringence will be applicable qualitatively to turbulent flow studies in two dimensions, particularly in boundary layer studies. Whether quantitative studies can also be made is uncertain since no specific relationships are known. Similarly its application to three-dimensional flow problems will depend primarily in developing the proper relationships, either analytically or experimentally.

ACKNOWLEDGMENT

The author wishes to express his gratitude to Dr. E.H. Kennard of the David Taylor Model Basin for his invaluable guidance and suggestions.

REFERENCES

1. Farwell, H.W., "Double Refraction in Colloidal Solutions," Journ. of Appl. Physics, Vol. 8, June 1937, pp. 416-417.

2. Kuhn, W., "Dehnungsdoppelbrechung von Kolloiden in Lösung," Zeit. f. Physik. Chemie, Vol. 161, No. 6, October 1932, pp. 427-440.

3. Leaf, W., "Fluid Flow Study of Locomotive Firebox Design," Mechanical Engineering, September 1945, pp. 586-590.

4. Alcock, E.D., and Sadron, C.L., "An Optical Method for Measuring the Distribution of Velocity Gradients in a Two-Dimensional Flow," Physics, Vol. 6, March 1935, pp. 92-95.

5. Rosset, A.J. de, "Double Refraction of Flow Studies with Methyl Methacrylate Polymers in Solution," Journ. of Chem. Physics, Vol. 9, October 1941, pp. 766-774.

6. Hauser, E.A., and Dewey, D.E., "Study of Liquid Flow," Ind. and Eng. Chem., Vol. 31, No. 6, June 1939, p. 786.

7. Hauser, E.A., and Lynn, J.E., "Separation and Fractionation of Colloidal Systems," Ind. and Eng. Chem., Vol. 32, No. 5, May 1940, pp. 659-662.

8. Hauser, E.A., and Reed, C.E., "Studies in Thixotropy. II - The Thixotropic Behavior and Structure of Bentonite," Journ. of Phys. Chem., Vol. 41, October 1937, pp. 911-934.

9. Hauser, E.A., and Schachman, "Particle Size Determination of Colloidal Systems by the Supercentrifuge," Journ. of Phys. Chem., Vol. 44, 1940, pp. 584-591.

10. Ambrose, H.A., and Loomis, A.G., "Some Colloidal Properties of Bentonite Suspensions," Physics, Vol. 1, August 1931, pp. 129-136.

11. Hauser, E.A., "Colloidal Phenomena," McGraw-Hill Book Co., New York, 1939.

12. M.I.T. Letter Report to DTMB under file L5-2(155), dated 11 December 1941.

13. Hatschek, E., "The Viscosity of Liquids," Van Nostrand Co., New York, 1928.

14. Ambrose, H.A., and Loomis, A.G., "Fluidities of Thixotropic Gels: Bentonite Suspensions," Physics, Vol. 4, No. 8, August 1933, pp. 265-273.

15. Mukherjee, J.H., Sen Gupta, N.C., and Sen, K.C., "Methods of Measuring Yield Value, Viscosity and Thixotropy," Indian Journ. of Physics, Vol. 16, February 1942, pp. 54-65.

16. Hoover, C.R., Putman, F.W., and Wittenberg, E.G., "The Depolarization of the Tyndall-Scattered Light of Bentonite and Ferric Oxide Sols," Journ. of Phys. Chem., Vol. 46, 1942, pp. 81-93.

17. Hauser, E.A., and LeBeau, D.S., "Studies in Colloidal Clays. II" Journ. of Phys. Chem., Vol. 45, 1941, pp. 54-65.

18. Robinson, J.R., "Studies in the Viscosity of Colloids," Proc. Roy. Soc. (London), Series A, Vol. 170, April 1939, pp. 519-550.

19. Mueller, H., and Sakmann, B.W., "Electro-Optical Properties of Colloids," Journ. of the Optical Soc. of America, Vol. 32, No. 6, June 1942, pp. 309-317.

20. Frocht, M., "Photoelasticity," Vol. I, John Wiley and Sons, New York, 1941.

21. Havelock, T.H., "Artificial Double Refraction, Due to Aeolotropic Distribution, with Application to Colloidal Solutions and Magnetic Fields," Proc. Roy. Soc. (London), Series A, Vol. 77, 1906, pp. 170-182.

22. Pfeiffer, H., "Über Strömungsdoppelbrechung und Doppelbrechung von Herapathit-Suspensionen," Koll. Zeit., Vol. 92, No. 2, August 1940, pp. 182-188.

23. Weller, R., Middlehurst, D.J., and Steiner, R., "The Photoviscous Properties of Fluids," NACA Tech. Note No. 841, February 1942.

24. Taylor, G.I., "The Formation of Emulsions in Definable Fields of Flow," Proc. Roy. Soc. (London), Series A, Vol. 146, October 1934, pp. 501-523.

25. Raman, C.V., and Krishman, K.S., "A Theory of the Birefringence Induced by Flow in Liquids," Phil. Mag., Serial 7, Vol. 5, No. 30, April 1928, pp. 769-783.

26. Edsall, J.T., "Streaming Birefringence and Its Relation to Particle Size and Shape," from "Advances in Colloid Science" Vol. I, International Publishers, New York, 1942, pp. 269-316.

27. Jeffery, G.B., "The Motion of Ellipsoidal Particles Immersed in a Fluid," Proc. Roy. Soc. (London), Series A, Vol. 102, 1923, pp. 161-179.

28. Burgers, J.M., from "Second Report in Viscosity and Plasticity," North Holland Publishers, Amsterdam, 1938, pp. 134-140.

29. Boeder, P., "Über Strömungsdoppelbrechung," Zeits. f. Physik, Vol. 75, 1932, pp. 258-281.

30. Langmuir, I., "The Role of Attractive and Repulsive Forces in the Formation of Tactoids, Thixotropic Gels, Protein Crystals and Coacervates," Journ. of Chem. Physics, Vol. 6, December 1938, pp. 873-896.

31. Marshal, C.E., "Studies in the Degree of Dispersion of the Clays. IV - The Shapes of Clay Particles," Journ. of Phys. Chem., Vol. 45, 1941, pp. 81-93.

32. Buchheim, W., Stuart, H.A., and Menz, H.Z., "Experimentelle Untersechungen der Strömungsdoppelbrechung Molekular Flüssigkeiten," Zeits. f. Physik, Vol. 112, No. 7-8, 1939, pp. 407-419.

33. Edsall, J.T., et al, "Studies on Double Refraction of Flow," Rev. of Sci. Inst., Vol. 15, No. 10, October 1944, p. 243.

34. Sadron, C., "Sur la Birefringence dynamique des Liquides purs," Journ. de Phys. et Rad., Series 7, Vol. 7, No. 6, 1936, pp. 263-269.

35. Foster, T.F., and Edsall, J.T., "Studies on Double Refraction of Flow. II. The Molecular Dimensions of Zein," Journ. of the Amer. Chem. Soc., Vol. 67, April 1945, pp. 617-625.

36. Snellman, O., and Bjornstahl, Y., "Einige Untersuchungen über Strömungsdoppelbrechung," Upsala, Kolloid-Bechefte, Vol. 52, No. 11/12, 1941, pp. 403-446.

37. Dewey, D.R. II, "Visual Studies of Fluid Flow Patterns Resulting from Streaming Double Refraction," M.I.T. Doctor's thesis, Dept. of Chem. Eng., 1941.

38. Rouse, H., "Fluid Mechanics for Hydraulic Engineers," McGraw-Hill Book Co., New York, 1938.

39. Wendt, F., "Turbulente Strömung Zwischen Zwei rotierenden Koaxialen Zylindern," Ingen.-Archiv, Vol. 4, 1933, pp. 577-595.

40. Page, L., "Introduction to Theoretical Physics," D. Van Nostrand Co., New York, August 1935.

41. Taylor, G.I., "Stability of a Viscous Liquid Contained between Two Rotating Cylinders," Phil. Trans., Series A, Vol. 223, February 1923, pp. 289-343.

42. Taylor, G.I., "Distribution of Velocity and Temperature between Concentric Rotating Cylinders," Proc. Roy. Soc. (London), Series A, Vol. 151, No. 874, October 1, 1935, pp. 494-512.

43. Wattendorf, F.L., "Effect of Curvature on Fully Developed Turbulent Flow," Proc. Roy. Soc. (London), Series A, Vol. 148, February 1935, pp. 565-598.

44. Pai Shih I, "Turbulent Flow between Rotating Cylinders," NACA Tech. Note No. 892, March 1943.

45. Weller, R., and Bussey, J.K., "Photoelastic Analysis of Three-Dimensional Stress Systems Using Scattered Light," NACA Tech. Note No. 737, November 1939.